Available online at www.sciencedirect.com
ScienceDirect
Trans. Nonferrous Met. Soc. China 26(2016) 1259−1268
Transactions of Nonferrous Metals Society of China
www.tnmsc.cn

Microstructures and mechanical properties of 2024Al/Gr/SiC hybrid composites fabricated by vacuum hot pressing

Cheng-jin HU[1,2], Hong-ge YAN[1,2], Ji-hua CHEN[1,2], Bin SU[1,2]

1. College of Materials Science and Engineering, Hunan University, Changsha 410082, China;
2. Hunan Provincial Key Laboratory of Spray Deposition Technology & Application, Hunan University, Changsha 410082, China

Received 23 April 2015; accepted 31 October 2015

Abstract: The 2024Al/Gr/SiC hybrid composite plates with 5%−10% SiC particles (volume fraction) and 3%−6% flaky graphite (Gr) (volume fraction) were fabricated by vacuum hot pressing and hot extrusion processing. The effects of SiC and Gr on the microstructures and mechanical properties of the composites aged at 160, 175 and 190 °C were studied by optical microscopy, scanning electron microscopy (SEM), and hardness and tensile tests. The results indicate that the SiC particles have a more obvious effect on accelerating the aging response as compared with the Gr. Both the tensile strength and elongation are reduced by the Gr and SiC particles added into the matrix, while the Gr has a more negative influence on the elongation than the SiC particles. The tensile strength (σ_b), yield stress (σ_s) and elongation (δ) of the 2024Al/3Gr/10SiC composite aged at 165 °C for 8 h are 387 MPa, 280.3 MPa and 5.7%, respectively. The hybrid composites are characterized by ductile fracture, which is associated with the ductile fracture of the matrix and the tearing of the interface between the matrix and the particles.
Key words: 2024Al/Gr/SiC composites; vacuum hot pressing; microstructure; mechanical property; heat treatment

1 Introduction

The 2024Al/SiC composite has significant applications in aerospace, weapons, automobile industries, etc., due to its high specific stiffness, strength and high elasticity modulus [1−3]. Mechanical properties of the 2024Al/SiC composite can be significantly improved by suitable heat treatment through aging hardening effect of the precipitates of S(Al_2CuMg) and θ(Al_2Cu) phases [4].

Generally, most metal matrix composites reinforced with ceramic particles are fabricated by the techniques such as squeeze or stir casting [5,6], spray forming [7] and power metallurgy [8,9]. However, the agglomeration, inclusions, non-uniform distribution and poor interface bonding associated with these techniques deteriorate the mechanical properties of the fabricated composites [5−9]. In order to overcome the above problems, some researchers [10,11] have utilized vacuum hot pressing to manufacture aluminum alloy matrix composites. The plastic deformation during hot pressing can break the oxide films of the alloy particles, so metallurgical bonding can be induced. Moreover, the relatively low preparation temperature suppresses the interfacial reaction between alloy matrix and reinforcement particles. This phenomenon is beneficial to the improvement of mechanical properties.

In recent years, damping has been regarded as a critical property for vibration reduction in both civilian and defense industries. High damping allows undesirable noise and vibration to be passively attenuated and removed to the surroundings as heat, which can reduce stress and increase fatigue life [12]. As a vital structure material used in the aerospace and automobile industries, a considerable effort has been made to improve the damping capacity of aluminum alloy matrix composites. Some researches [12−15] indicate that a reasonable addition of flaky graphite into the composite can improve the damping capacity, but the mechanical properties of composites decrease with the addition of graphite (Gr) flakes. This degradation restricts the application of the composites reinforced by Gr in the industries because the structure materials require higher mechanical properties. There are almost no reports available about the effect of flaky graphite on the

Corresponding author: Hong-ge YAN; Tel: +86-731-88821727; Fax: +86-731-88823554; E-mail: yanhg68@163.com
DOI: 10.1016/S1003-6326(16)64226-7

mechanical properties of 2024Al/Gr/SiC hybrid composite.

Therefore, the present study is aimed to study the effects of flaky graphite and SiC particles on the microstructures and mechanical properties of 2024Al/Gr/SiC hybrid composites. The aging characteristics of 2024Al and 2024Al/Gr/SiC hybrid composites are studied using hardness tests.

2 Experimental

2.1 Material and methods

The chemical composition of the inert gas atomizing powders of 2024Al alloy consists of 3.53% Cu, 1.28% Mg, 0.2% Fe, 0.04% Si and balance aluminum (mass fraction). The SEM images of the 2024Al powders, commercially available SiC powders with the average size of 7.5 μm and the flaky graphite are shown in Fig. 1. Five kinds of materials were prepared as follows: 2024Al, 2024Al/3%Gr (2024Al/3Gr), 2024Al/6%Gr (2024Al/6Gr), 2024Al/3%Gr/5%SiC (2024Al/3Gr/5SiC), 2024Al/3%Gr/10%SiC (2024Al/3Gr/10SiC) (volume fraction).

The composite plates were prepared by vacuum hot pressing of the mixtures of 2024Al powders, SiC powders and flaky graphite. The SiC particles have been calcined at 900 °C for 3 h before mixing. The whole processes are shown in Fig. 2. The mixed powders containing 2024Al, SiC and Gr were mixed for 3 h in a VH8-V-shaped mixer and then heated at 170 °C for 1 h with argon shielding to remove the moisture. Then, the uniformly mixed powders were packed in the moisture proof aluminum foil bags with 110 mm in diameter and 700 mm in depth, followed by vacuum treating for 1.5 h. Cold compaction was conducted on a YJ32−315A four-column hydraulic press at a pressure of 390 MPa for 2.5 h to form a solid green compact. The solid green compact was hot-pressed at 490 °C with a tolerance of ±3 °C at a pressure of 390 MPa for 0.5 h. Finally, the hot-pressed composite with a size of *d*100 mm × 60 mm was extruded into plate with a section size of 40 mm × 10 mm at an extrusion ratio of 22:1 after soaking at 470 °C for 0.5 h. The as-extruded composite samples were solution-treated at (515±3) °C for 0.5 h, and then rapidly quenched in cold water. Aging treatment was performed at 160, 175 and 180 °C, respectively, with a tolerance of ±1 °C for 0.25 to 24 h.

2.2 Characterization

The Brinell hardness was measured on an HBRV−187.5 hardness tester at a load of 612.9 N. At least five measurements were recorded for each samples and averaged. The peak-aged samples were machined into flat tensile specimens with a gauge section of 17 mm × 4 mm × 2 mm. The tensile tests were carried out on an Instorn3369 testing machine with an initial strain rate of 0.5×10^{-3} s^{-1} at room temperature. The tensile strength (σ_b), yield stress (σ_s) and elongation (δ) are averaged over three samples. The morphologies of powders and tensile fracture were observed by scanning electron microscopy (SEM, Hitachi S−4800). An optical microscope (Carl Zeiss-Axio Lab.A1) was used to examine the microstructures of the composite samples.

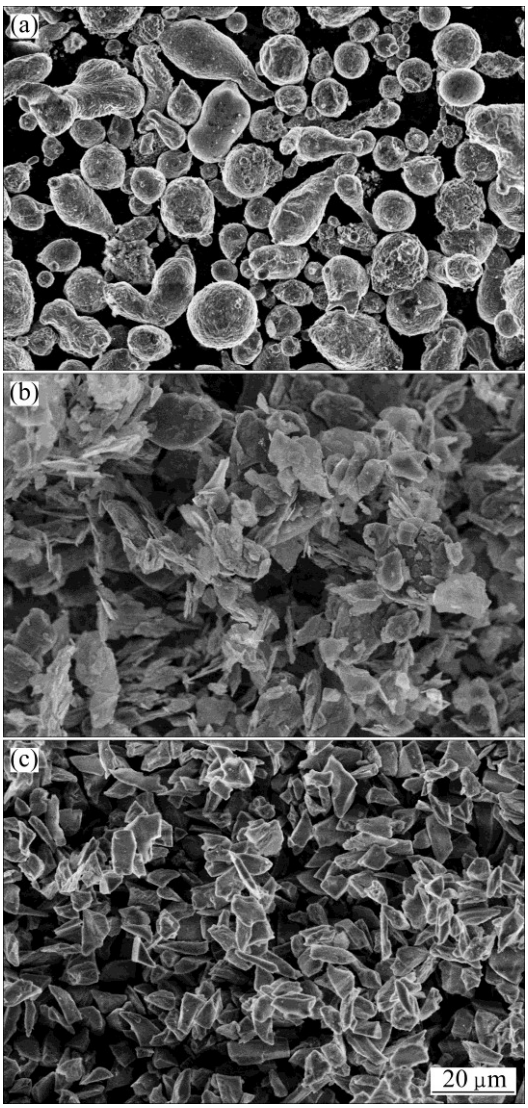

Fig. 1 SEM images of 2024Al powders (a), SiC particles (b), and flaky graphite (c)

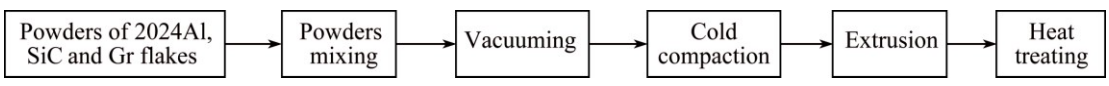

Fig. 2 Flow diagram of preparation process of composite plates

3 Results and discussion

3.1 Microstructure

The microstructures of the peak-aged composites along the extrusion direction are shown in Fig. 3. As seen from Fig. 3(a), the 2024Al particles are stretched along the extrusion direction, and the boundaries between the particles are not observed after extrusion deformation. Moreover, the recrystallized grains are too small to be distinguished.

The microstructure of 2024Al/3Gr is shown in Fig. 3(b). It is noticeable that the flaky graphite particles are uniformly distributed in a stream line state. This is due to the flowing of the flaky graphite with the matrix during the extrusion deformation. Figure 4(a) shows the irregular interface between the graphite and the matrix, which is due to lower strength of graphite than that of the matrix. But no obvious porosities are detected. A certain amount of flaky graphite may be served as solid lubricant to decrease the density gradient so that the density of composite is increased by promoting more uniform pressure transmission [16−19]. The densification mechanisms during cold compaction are the rearrangement of power particles and the plastic deformation of soft particles, such as flaky graphite [10,20]. In other words, the deformation of flaky graphite at great pressure can improve the bonding between the Gr flakes and the matrix.

The microstructure of 2024Al/6Gr is shown in Fig. 3(c), which shows the reasonable inhomogeneous distribution of flaky graphite and clusters in some regions due to the high volume fraction of flaky graphite up to 6%. This is possibly related to the increasing interface contact between the flaky graphite and the matrix. However, almost no porosity is observed in the samples due to the lubricating effect of flaky graphite, which is quite different from the previous report [21].

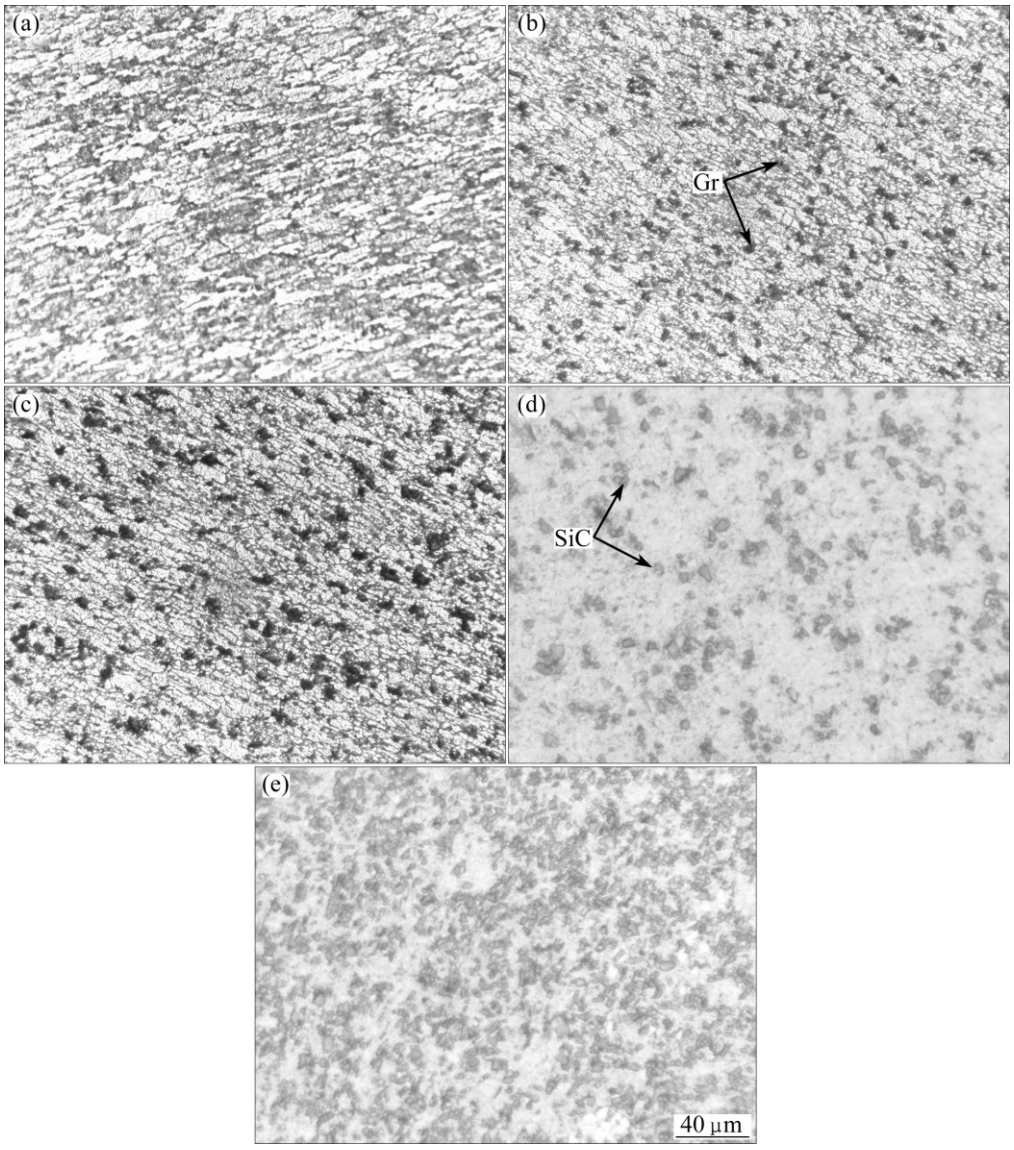

Fig. 3 Microstructures of composites: (a) 2024Al; (b) 2024Al/3Gr; (c) 2024Al/6Gr; (d) 2024Al/3Gr/5SiC; (e) 2024Al/3Gr/10SiC

Figures 3(d) and (e) show the microstructures of the 2024Al/3Gr/5SiC and 2024Al/3Gr/10SiC composites, respectively. It is noted that the SiC particles are relatively uniformly distributed in the matrix. Close interfaces combination between the SiC particles and the matrix is observed and only few individual small pores are remained between the SiC particle agglomerates (Fig. 4(b)). Therefore, the hot pressing combined with hot extrusion plays a significant role in improving the combination between the hybrid particles and the alloy matrix.

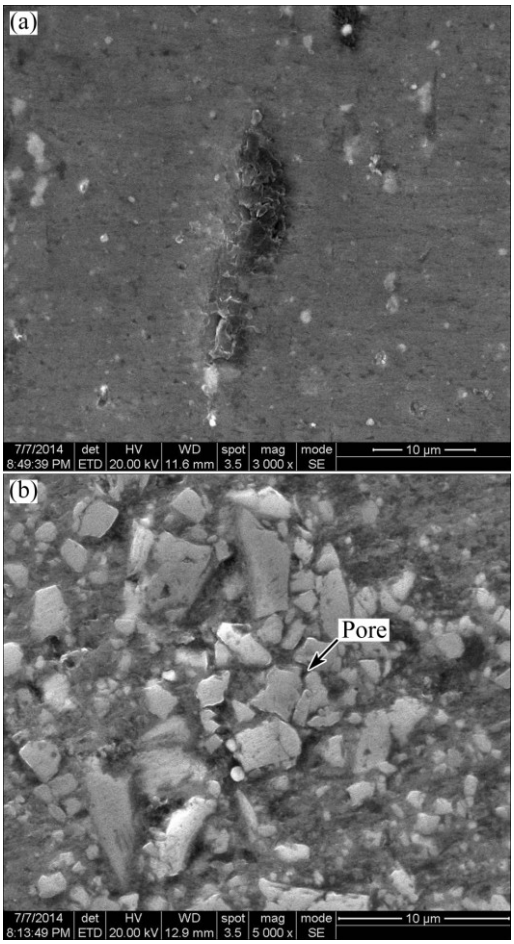

Fig. 4 SEM images of Gr/matrix interface (a) and SiC/matrix interface (b)

3.2 Mechanical properties

3.2.1 Hardness

The variation of the hardness of 2024Al alloy and 2024Al/Gr/SiC hybrid composites with aging time at different temperatures is shown in Fig. 5.

Figure 5 shows the rapid initial hardening of both 2024Al and 2024Al/Gr/SiC hybrid composites aged at 160, 175 and 190 °C. After that, the hardness of 2024Al and 2024Al/Gr/SiC hybrid composites increases at a slower rate until reaches the peak hardness. Then, the hardness decreases with increasing the aging time, possibly due to an over aging effect. This is consistent with the previous reports [22−25]. The extremely rapid initial hardening reaction is attributed to the formation of Cu−Mg co-clusters.

As shown in Figs. 5(a)−(f), the time for peak aging decreases with increasing the aging temperature. This is to be expected since higher temperature accelerates the precipitation rate of second phases and leads to a rapid aging response. The comparison of aging curves of the 2024Al and composites containing 3% Gr and 6% Gr at 175 °C is shown in Fig. 5(c). The decrease of peak aging time with the increase of Gr content can be seen by comparing 2024Al with 2024Al/6Gr. But 3% graphite added to the matrix does not accelerate the aging response as compared 2024Al with 2024Al/3Gr, which is similar with the previous study [26]. PAL et al [26] found that the peak-aging hardness values of the Al−Cu−Mg/SiC composites were higher and the peak aging time was 1 h longer than those of the matrix. This phenomenon can be explained by the following three aspects. Firstly, the Gr flakes lead to a reduction in the volume fraction of the GP zones, which is due to lower vacancy concentration in the composite than that in 2024Al alloy sample. It is believed that the large area of the particle/matrix interface, acting as the vacancy sinks, should be responsible for lower vacancy concentration in the composites. The formation of the GPB zones, which is regarded as the main factor affecting the remaining steps of the aging sequence, may be retarded due to lower vacancy concentration in the composite in comparison with that in the alloy [27,28]. Secondly, in addition to the deformability of the Gr fakes, the addition of Gr flakes has no obvious effect on the dislocation density of the matrix for the slight difference between the coefficients of thermal expansion of the Gr particles and the 2024Al matrix. Thirdly, the Gr/Al interfaces act as the heterogeneous nucleation sites, which accelerate the precipitation rate of the second phase and shorten the aging time to get the peak hardness. Therefore, the aging behavior of the composites depends on the competition between the dislocation density generated and the availability of vacancy in the composites. Higher dislocation density induced by the particles is expected to accelerate the aging response. However, the particle/matrix interface acts as a vacancy sink, so that the vacancies diffuse to the surface of the particles. These vacancies fail to contribute to heterogeneous nucleation of precipitates. In comparison with the peak hardness of 2024Al, 2024Al/3Gr and 2024Al/6Gr, it is found that higher volume fraction of the Gr particles results in lower peak aging hardness, which is attributed to lower hardness of the Gr particles.

The hardness data as a function of aging time for the 2024Al/3Gr, 2024Al/3Gr/5SiC and 2024Al/3Gr/10SiC composites are plotted in Figs. 5(b), (d) and (f).

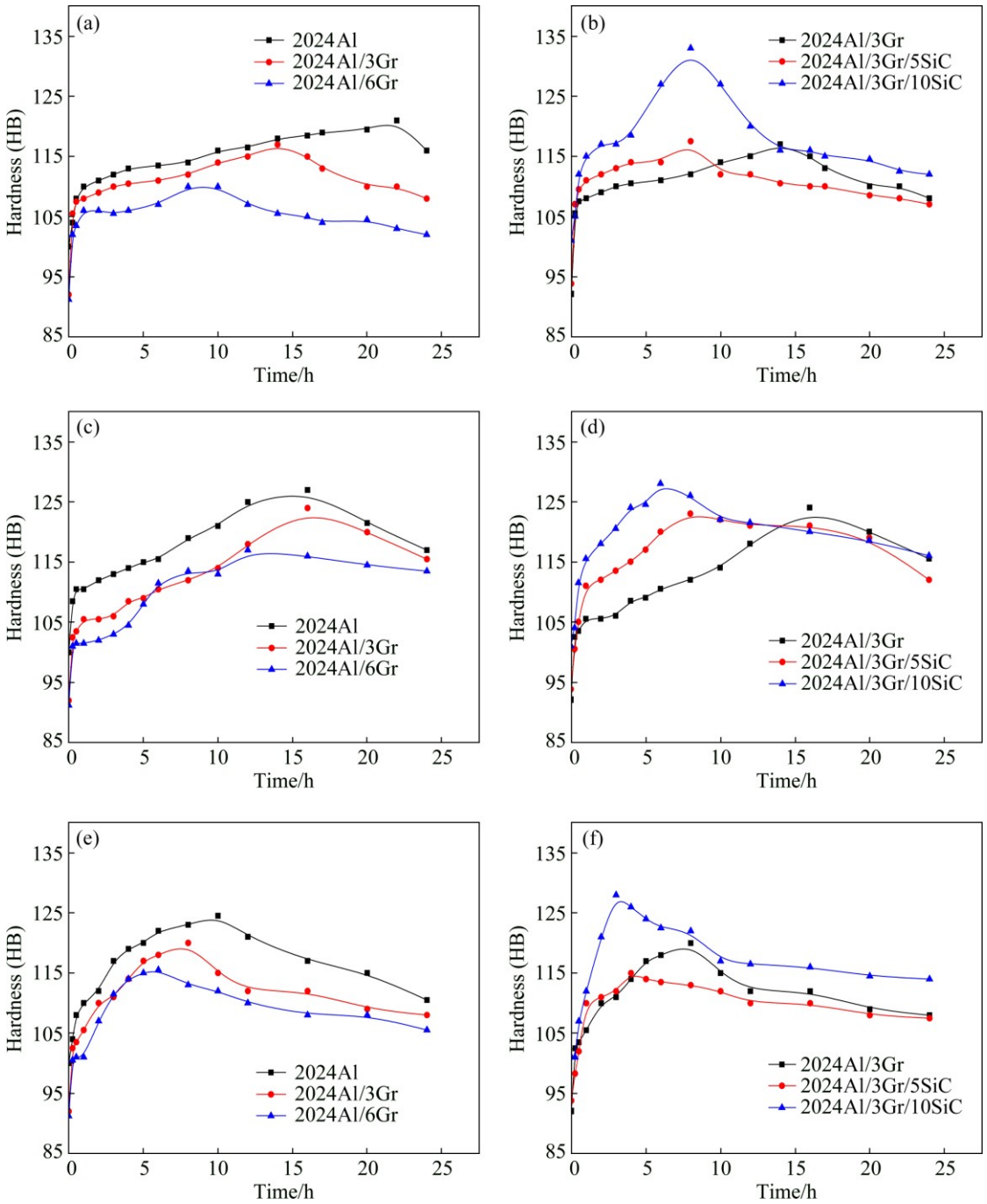

Fig. 5 Variation of Brinell hardness (± HB 1.5) in samples annealed at different temperatures: (a, b) 160 °C; (c, d) 175 °C; (e, f) 190 °C (Solution treatment was carried out at 515 °C for 0.5 h)

Note that the peak aging time is obviously shortened by the addition of SiC particles in 2024Al/3Gr composite. Moreover, as the volume fraction of SiC increases, the peak hardness increases. Similar results were reported by the previous studies [29,30]. Higher dislocation density can be induced by the hard SiC particles because of the large mismatch in the thermal expansion coefficient between the matrix and SiC particles. Higher dislocation density promotes the diffusion of alloying elements, which leads to higher nucleation and growth rate of the precipitates [30,31]. SiC particles act as efficient barriers to dislocation movement and this is different from the graphite flakes. These effects may contribute to accelerating the aging response. In addition, the aging kinetic is also promoted by the possibility of heterogeneous nucleation of metastable phases on the SiC/matrix interface [32].

3.2.2 Tensile properties

The tensile properties of composites in the peak aging state are shown in Fig. 6 and Table 1.

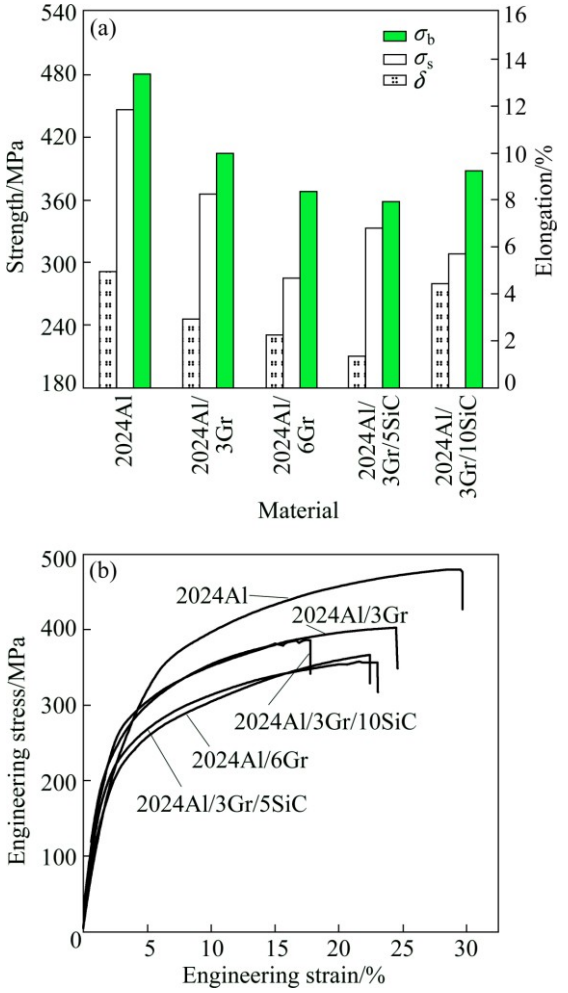

Fig. 6 Tensile properties of samples at peak aging time: (a) Comparison of tensile properties; (b) Tensile curve

Table 1 Tensile properties of 2024Al/Gr/SiC composites

Material	σ_b/MPa	σ_s/MPa	δ/%
2024Al	480.2±6.4	290.7±5.3	11.8±1.0
2024Al/3Gr	402.9±9.7	245.1±8.9	8.2±1.4
2024Al/6Gr	367.6±8.2	230.7±10.1	4.6±1.3
2024Al/3Gr/5SiC	358.4±7.4	208.8±8.5	6.8±0.7
2024Al/3Gr/10SiC	387±5.3	280.3±6.1	5.7±0.9

The 2024Al alloy exhibits the best mechanical properties, as shown in Fig. 6(a). The strength and elongation of the composites with Gr flakes decrease with increasing the volume fraction of Gr in the 2024Al matrix. As the SiC particles were added into the 2024Al/3Gr composite, the strength shows a slight decrease and then an increase. However, the elongation increases firstly and then decreases. The σ_b, σ_s and δ of 2024Al/3Gr/10SiC are 387 MPa, 280.3 MPa and 5.7%, respectively. Similar results were reported by PRASAD et al [33] who investigated the effect of reinforcement particles on the mechanical properties of aluminum hybrid composites fabricated by double stir casting. They found that the tensile strength and yield stress increased with the increase of mass fraction of the reinforcement particles, whereas the elongation decreased with the increase of the reinforcements. The tensile strength, yield stress and elongation of A356.2/8%RHA (rice husk ash)/8%SiC hybrid composite were 356MPa, 258MPa and 4.9%, respectively.

As indicated above, the Gr has a greater impact on the elongation of the composites than the SiC. This can be attributed to the formation of a coherent layer of SiO_2 on the surface of SiC particles due to roasting. The SiO_2 coherent layer is expected to protect the SiC from aluminum attack and improve the wettability of SiC particles in alloy matrix [34]. The interfacial reactions between the SiO_2 layer and the reactive elements (such as Mg, Ti) are conducive to good metallurgical bonding interface [34]. However, compared with the SiC/Al interface, the Gr/Al interface is weaker due to the interfacial reactions between the Gr and the Al matrix [35].

Assuming that the Gr and SiC particles can be equiaxed, the spacing between particles (λ) is calculated by the equation $\lambda=0.77d\varphi_p^{-1/2}$, in which d is the particle size and φ_p is the volume fraction of particles [36]. According to this equation, the spacing between particles decreases exponentially with increasing the volume fraction of particles, which is responsible for the matrix being dramatically divided by the particles. Thus, the σ_b and σ_s decrease with increasing the volume fractions of SiC and Gr. In addition, the Gr particles are known as crack initiation sources in the composites due to the weak van der Waals force between the Gr interlayers and the weak interfacial bonding between the Al matrix and the Gr particles [37]. According to the explanation mentioned above, the fact that the 2024Al/3Gr/10SiC composite has higher strength than the 2024Al/3Gr/5SiC composite is attributed to the following competitive processes. On the one hand, increasing the volume fraction of particles leads to smaller particle spacing and introduces more porosities which deteriorate the mechanical properties of composites. On the other hand, the dislocation density in the matrix increases with increasing the volume fraction of particles.

3.3 Fracture analysis

The typical SEM tensile fracture images of 2024Al, 2024Al/3Gr, 2024Al/6Gr, 2024Al/3Gr/5SiC and 2024Al/3Gr/10SiC samples are shown in Fig. 7. It can be seen from Figs. 7(a) and (b) that the fracture surfaces of the 2024Al sample reveal a typical dimple morphology. The dimples are known to be created by nucleation, growth and coalescence of micro-voids during tensile deformation.

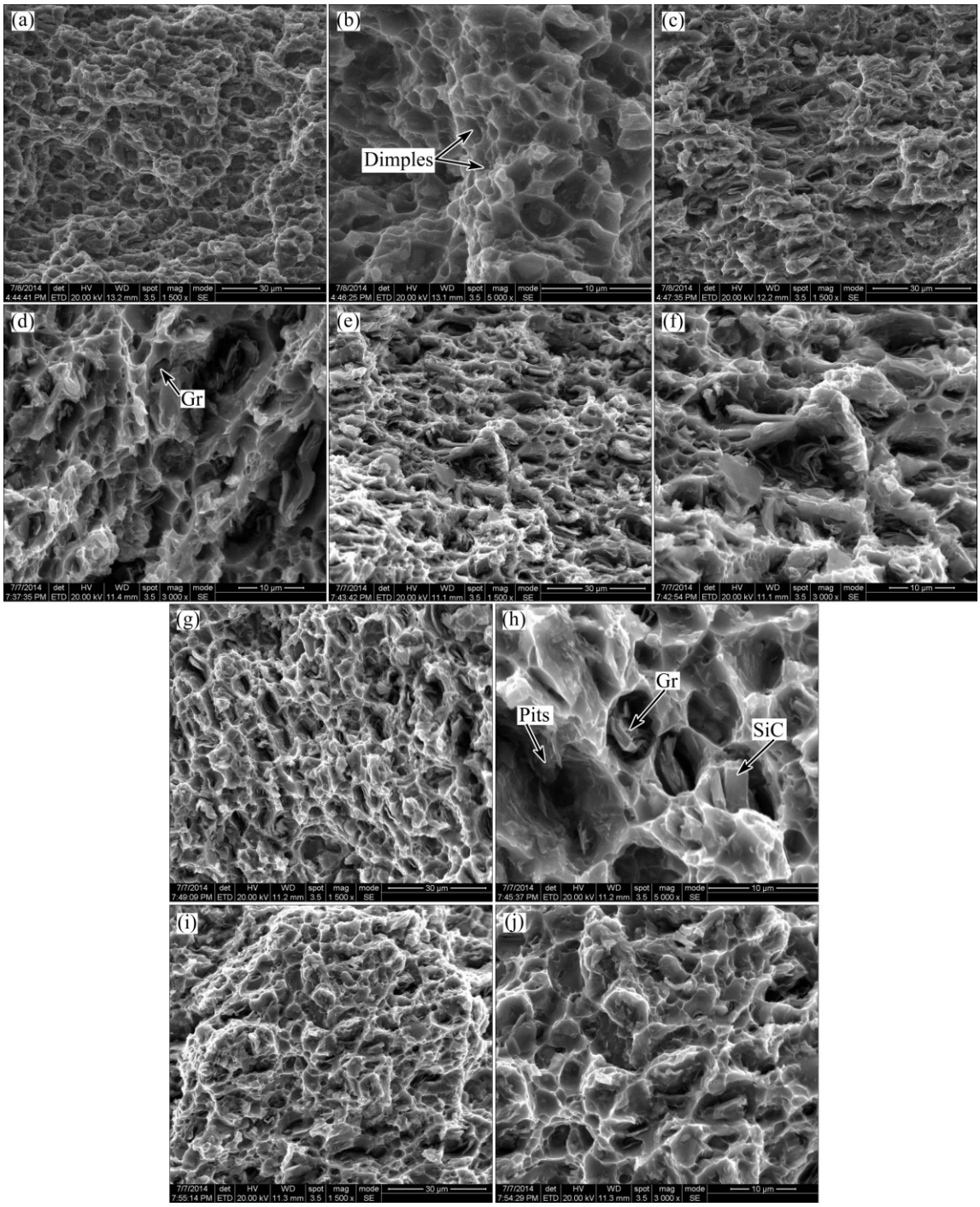

Fig. 7 SEM images of fracture surface of 2024Al (a, b), 2024Al/3Gr (c, d), 2024Al/6Gr (e, f), 2024Al/3Gr/5SiC (g, h), 2024Al/3Gr/10SiC (i, j)

The facture surfaces of the composites are quite different from that of the alloy matrix. Figures 7(c)−(f) show the fracture surfaces of flaky graphite and debonding between Gr particles and the matrix in the Gr clusters area in the 2024Al/3Gr and 2024Al/6Gr composites. Moreover, dimples are also detected in the 2024Al/3Gr and 2024Al/6Gr samples, which are attributed to the coalescence of micro-voids.

As can be seen from Figs. 7(g)−(j), the facture surfaces of the 2024Al/3Gr/5SiC and 2024Al/3Gr/10SiC composites exhibit the similar features. The pits existing in the matrix are caused by the pulling-out of the reinforcing particles from the matrix. Moreover, the pits are featured mainly by the size and distribution of the reinforcing particles, which indicates that the rupture of 2024Al/3Gr/5SiC and 2024Al/3Gr/10SiC composites is mainly caused by the pulling-out of SiC particles. The residual cracked Gr particles are found in the matrix. The

Gr particles tend to rupture rather than pulling-out due to the weak van der Waals forces between the Gr interlayers. In addition, there is only a small fraction of fracture surface that is dominated by small dimples. These small dimples are generally distributed at the boundaries between the fits, probably due to the ductile rupture of the aluminum matrix.

4 Discussion

It can be found that the 2024Al powders are stretched along the extrusion direction and no obvious boundaries between the particles are observed after extrusion deformation (Fig. 3(a)). The flaky graphite powders added into the composite are uniformly distributed in a streamline state (Fig. 3(b)). Moreover, no obvious porosities are found. A certain amount of flaky graphite may served as solid lubricant to decrease the density gradient so that the density of composite is increased by promoting more uniform pressure transmission [16−18]. With increasing the volume fraction of Gr, clusters and reasonable inhomogeneous distribution of flaky graphite occur in some regions (Fig. 3(c)) due to the increased interface contact between the graphites. No evident clusters are examined in 2024Al/3Gr/5SiC and 2024Al/3Gr/10SiC composites. In other words, the additions of 5% SiC and 10% SiC are both relatively uniformly distributed in the matrix (Figs. 3(d) and (e)). The Gr and SiC particles have an obvious effect on the fracture. The 2024Al shows a dimple morphology. However, the fracture of composites is characterized by the fracture of flaky graphite and the tearing of the Gr/matrix interface and SiC/matrix interface.

The tensile properties decrease with increasing the volume fraction of Gr powers because the Gr flakes are known as crack initiation sources in the composite due to the weak van der Waals forces between the Gr interlayers and the weak interfacial bonding between the Al matrix and the Gr particles [37]. The tensile strength and yield stress increase with increasing the volume fraction of SiC particles, while the elongation shows a decrease as the volume fraction of SiC particles increases. The increase of strength of the composites is probably due to the increase of dislocation density [33].

5 Conclusions

1) The 2024Al/Gr/SiC hybrid composite plates were fabricated by vacuum hot pressing. The hydrostatic pressure and shear deformation during hot pressing and extrusion eliminates the boundaries between the 2024Al powders and improve the interfacial bonding of Gr/matrix and SiC/matrix. The relative homogeneity of SiC and Gr within the matrix is achieved.

2) The precipitation of the second phases is accelerated by the addition of Gr and SiC. The SiC particles have a more significant effect than the Gr due to a greater mismatch in the thermal expansion coefficient between SiC particles and the matrix. This mismatch leads to a higher dislocation density in the composites. The time for the peak aging of the 2024Al/3Gr/10SiC at 190 °C is only 3 h.

3) The strength and elongation decrease with increasing the volume fractions of SiC particles and Gr added to the matrix. The Gr flakes have a greater negative impact on the elongation than the SiC particles due to weaker Gr/matrix interface. The σ_b, σ_s and δ of the 2024Al/3Gr composite are 420 MPa, 245 MPa and 9.6%, respectively, while those of the 2024Al/3Gr/10SiC composites are 387 MPa, 280.3 MPa and 5.7%, respectively.

4) The fracture mechanism of the 2024Al/SiC/Gr hybrid composites is ductile fracture, which is associated with the ductile fracture of the matrix and the tearing of the interface between the matrix and the particles.

Acknowledgements

The authors appreciate Pro. Shou-ren WANG of Central South University for the assistance in tensile testing and Pro. Jiang-hua CHENG of Hunan University for the assistance in SEM examination.

References

[1] ZHANG Fan, LI Xiao-cui, JIN Chen, HU Zheng-jun. Studies on microyield behavior of a SiC_p/2024Al composite [J]. Transactions of Nonferrous Metals Society of China, 1998, 8(3): 449−454.

[2] LIU Z Y, WANG Q Z, XIAO B L, MA Z Y, LIU Y. Experimental and modeling investigation on SiC_p distribution in powder metallurgy processed SiC_p/2024Al composites [J]. Materials Science and Engineering A, 2010, 527(21−22): 5582−5591.

[3] MURATOGLU M. Effect of heat treatments on failure, mechanism of SiC_p/2124-Al composite [J]. Transactions of Nonferrous Metals Society of China, 2005, 15(4): 839−845.

[4] ABARGHOUIE S M, REIHANI S S. Aging behavior of a 2024 Al alloy−SiC_p composite [J]. Materials and Design, 2010, 31(5): 2368−2374.

[5] WANG Yi-qi, SONG Jung-II. Dry sliding wear behavior of Al_2O_3 fiber and SiC particle reinforced aluminum based MMCs fabricated by squeeze casting method [J]. Transactions of Nonferrous Metals Society of China, 2011, 21(7): 1441−1448.

[6] SURESH S, MOORTHI N S V. Process development in stir casting and investigation on microstructures and wear behavior of TiB_2 on Al6061 MMC [J]. Procedia Engineering, 2013, 64: 1183−1190.

[7] SU Y H F, CHEN Y C, TSAO C Y. Workability of spray-formed

7075 Al alloy reinforced with SiC_p at elevated temperatures [J]. Materials Science and Engineering A, 2004, 364(1−2): 296−304.

[8] RAVINDRAN P, MANISEKAR K, NARAYANASAMY P, RATHIKA P. Tribological properties of powder metallurgy-processed aluminium self lubricating hybrid composites with SiC additions [J]. Materials and Design, 2013(45): 561−570.

[9] RAVINDRAN P, MANISEKAR K, NARAYANASAMY R, NARAYANASAMY P. Tribological behaviour of powder metallurgy-processed aluminium hybrid composites with the addition of graphite solid lubricant [J]. Ceramics International, 2013, 39(2): 1169−1182.

[10] HONG S H, CHUNG K H. Effects of vacuum hot pressing parameters on the tensile properties and microstructures of SiC−2124Al composites [J]. Materials Science and Engineering A, 1995, 194(2): 165−170.

[11] TAN Z Q, LI Z Q, FAN G L, KAI X Z, JI G, ZHANG L T, ZHANG D. Fabrication of diamond/aluminum composites by vacuum hot pressing: Process optimization and thermal properties [J]. Composites Part B: Engineering, 2013, 47: 173−180.

[12] PEREZ R J, ZHANG J, GUNGOR M N, LAVERNIA E J. Damping behavior of 6061Al/Gr metal matrix composites [J]. Metallurgical Transactions A, 1993, 24(3): 701−712.

[13] KUMAR H G P, XAVIOR M A. Graphene reinforced metal matrix composite (GRMMC): A review [J]. Procedia Engineering, 2014, 97: 1033−1040.

[14] GU J H, ZHANG X N, GU M Y, GU M, WANG X K. Internal friction peak and damping mechanism in high damping 6061Al/SiC_p/Gr hybrid metal matrix composite [J]. Journal of Alloys and Compounds, 2004, 372(1−2): 304−308.

[15] WU G H, DOU Z Y, JIANG L T. Damping properties of aluminum matrix−fly ash composites [J]. Materials Letters, 2004, 60(24): 2945−2948.

[16] NOR S S M, RAHMAN M M, TARLOCHAN F, SHAHIDA B, ARIFFIN A K. The effect of lubrication in reducing net friction in warm powder compaction process [J]. Journal of Materials Processing Technology, 2008, 207(1−3): 118−124.

[17] JIANG G, DAEHN G S, LANNUTTI J J, FU Y, WAGONER R H. Effects of lubrication and aspect ratio on the consolidation of metal matrix composites under cyclic pressure [J]. Acta Materialia, 2001, 49(8): 1471−1477.

[18] HUANG H S, LIN Y C, HWANG K S. Effect of lubricant addition on the powder properties and compacting performance of spray-dried molybdenum powders [J]. International Journal of Refractory Metals and Hard Materials, 2002, 20(3): 175−180.

[19] HAFIZPOUR H R, SANJARI M, SIMCHI A. Analysis of the effect of reinforcement particles on the compressibility of Al−SiC composite powders using a neural network model [J]. Materials and Design, 2009, 30(5): 1518−1523.

[20] POQUILLON D, LEMAITRE J, BACO-CARLES V, TAILHADES Ph, LACAZE J. Cold compaction of iron powders—Relations between powder morphology and mechanical properties: Part I: Powder preparation and compaction [J]. Powder Technology, 2002, 126(1): 65−74.

[21] MAHDAVI S, AKHLAGHI F. Effect of SiC content on the processing, compaction behavior, and properties of Al6061/SiC/Gr hybrid composites [J]. Journal of Materials Science, 2011, 46(5): 1502−1511.

[22] AIGBODION V S. Thermal ageing on the microstructures and mechanical properties of Al−Cu−Mg alloy/bagasse ash particulatecomposites [J]. Journal of King Saud University: Engineering Sciences, 2014, 26(2): 144−151.

[23] RINGER S P, HONO K, SAKURAI T, POLMEAR I J. Cluster hardening in an aged Al−Cu−Mg alloy [J]. Scripta Materialia, 1997, 36(5): 517−521.

[24] RINGER S P, SAKURAI T, POLMEAR I J. Origins of hardening in aged Al−Cu−Mg (Ag) alloys [J]. Acta Materialia, 1997, 45(9): 3731−3744.

[25] RINGER S P, HONO K, SAKURAI T, POLMEAR I J, SAKURAI T. Precipitation processes during the early stages of ageing in Al−Cu−Mg alloys [J]. Applied Surface Science, 1996, 94−95: 253−260.

[26] PAL S, MITRA R, BHANUPRASAD V V. Aging behaviour of Al−Cu−Mg alloy−SiC composites [J]. Materials Science and Engineering A, 2008, 480(1−2): 496−505.

[27] THOMAS M P, KING J E. Comparison of the ageing behaviour of PM 2124 Al alloy and Al−SiC_p metal-matrix composite [J]. Journal of Materials Science, 1994, 29(20): 5272−5278.

[28] JANOWSKI G M, PLETKA B J. The effect of particle size and volume fraction on the aging behavior of a liquid-phase sintered SiC/aluminum composite [J]. Metallurgical and Materials Transactions A, 1995, 26(11): 3027−3035.

[29] SURESHA S, SRIDHARA B K. Effect of silicon carbide particles on wear resistance of graphitic aluminum matrix composites [J]. Materials and Design, 2010, 31(9): 4470−4477.

[30] PARVIN N, ASSADIFARD R, SAFARZADEH P, SHEIBANI S, MARASHI P. Preparation and mechanical properties of SiC-reinforced Al6061 composite by mechanical alloying [J]. Materials Science and Engineering A, 2008, 492(1−2): 134−140.

[31] SALVO L, SUERY M, TOWLE D, FRIENSD C M. Age-hardening behaviour of liquid-processed 6061 alloy reinforced with particles and short fibres [J]. Composites Part A, 1996, 27(12): 1201−1210.

[32] SEYED REIHANIA S M. Processing of squeeze cast Al6061−30vol% SiC composites and their characterization [J]. Materials and Design, 2006, 27(3): 216−222.

[33] PRASAD D S, SHOBA C, RAMANAIAH N. Investigations on mechanical properties of aluminum hybrid composites [J]. Journal of Materials Research and Technology, 2014, 3(1): 79−85.

[34] SHI Z L, YANG J M, LEE J C, ZHANG D, LEE H I, WU R J. The interfacial characterization of oxidized $SiC_{(p)}$/2014 Al composites [J]. Materials Science and Engineering A, 2001, 303(1−2): 46−53.

[35] YANG H N, GU M Y, JIANG W J, ZHANG G D. Interface microstructure and reaction in Gr/Al metal matrix composites [J]. Journal of Materials Science, 1996, 7(31): 1903−1907.

[36] LEROY G, EMBURY J D, EDWARD G, ASHBY M F. A model of ductile fracture based on the nucleation and growth of voids [J]. Acta Metallurgica, 1981, 29(8): 1509−1522.

[37] LENG J F, WU G H, ZHOU Q B, DOU Z Y, HUANG X L. Mechanical properties of SiC/Gr/Al composites fabricated by squeeze casting technology [J]. Scripta Materialia, 2008, 59(6): 619−622.

真空热压法制备 2024Al/Gr/SiC 复合材料的显微组织和力学性能

胡程进[1,2]，严红革[1,2]，陈吉华[1,2]，苏 斌[1,2]

1. 湖南大学 材料科学与工程学院，长沙 410082；
2. 湖南大学 湖南省喷雾沉积技术与应用重点实验室，长沙 410082

摘 要：采用真空热压法制备了 2024Al/Gr/SiC 复合材料，其中 SiC 颗粒和鳞片状石墨(Gr)的体积分数分别为 5%~10%和 3%~6%。采用光学显微镜、扫描电镜、硬度和拉伸性能测试研究 SiC 颗粒和石墨对分别经 160、175 和 190 ℃ 时效处理后复合材料显微组织和力学性能的影响。结果表明：加入 SiC 颗粒和石墨能明显加速第二相时效析出，但 SiC 颗粒对时效行为的影响比石墨大。复合材料的拉伸强度和伸长率随着 SiC 颗粒和石墨含量的增加而降低，石墨对伸长率的影响比 SiC 颗粒更大。2024Al/3Gr/10SiC 复合材料在 165 ℃ 时效 8 h 时的抗拉强度、屈服强度和伸长率分别为 387 MPa，280.3 MPa 和 5.7%。2024Al/Gr/SiC 复合材料的断裂机制为基体韧性断裂和复合相颗粒与基体间撕裂断裂。

关键词：2024Al/Gr/SiC 复合材料；真空热压法；显微组织；力学性能；热处理

(Edited by Mu-lan QIN)